The Company of Biologists

RESEARCH ARTICLE

Traction reinforcement in prehensile feet of harvestmen (Arachnida, Opiliones)

Jonas O. Wolff[1,2,*], Chantal Wiegmann[1,3], Christian S. Wirkner[4], Alexander Koehnsen[1] and Stanislav N. Gorb[1]

ABSTRACT

Prehensile and gripping organs are recurring structures in different organisms that enhance friction by the reinforcement and redirection of normal forces. The relationship between organ structure and biomechanical performance is poorly understood, despite a broad relevance for microhabitat choice, movement ecology and biomimetics. Here, we present the first study of the biomechanics of prehensile feet in long-legged harvestmen. These arachnids exhibit the strongest sub-division of legs among arthropods, permitting extreme hyperflexion (i.e. curling up the foot tip). We found that despite the lack of adhesive foot pads, these moderately sized arthropods are able to scale vertical smooth surfaces, if the surface is curved. Comparison of three species of harvestmen differing in leg morphology shows that traction reinforcement by foot wrapping depends on the degree of leg sub-division, not leg length. Differences are explained by adaptation to different microhabitats on trees. The exponential increase of foot section length from distal to proximal introduces a gradient of flexibility that permits adaptation to a wide range of surface curvature while maintaining integrity at strong flexion. A pulley system of the claw depressor tendon ensures the controlled flexion of the high number of adesmatic joints in the harvestman foot. These results contribute to the general understanding of foot function in arthropods and showcase an interesting model for the biomimetic engineering of novel transportation systems and surgical probes.

KEY WORDS: Attachment, Friction, Adhesion, Arthropod leg, Wrap, Locomotion

INTRODUCTION

Traction on a surface is a critical condition of locomotion, and is predominantly governed by frictional and adhesion forces between animal and environmental surfaces. Friction and adhesion largely depend on short-ranging inter-molecular attractive forces and thus on the number of close contact points. As most biological surfaces are soft and deformable, the contact area depends on the magnitude of normal forces, i.e. the application of pressure. When walking on a horizontal surface, normal forces are exerted by body weight, but with increasing surface incline, this effect diminishes. Therefore, to scale vertical and overhanging surfaces, many animals, such as primates, birds, lizards, frogs and arthropods, enhance traction by

opposing friction or normal forces of contralateral toes or legs (Bußhardt et al., 2014; Endlein et al., 2017; Gladun and Gorb, 2007). On flat surfaces, the generation of high directional friction is often achieved by hooked claws and anisotropically microstructured surfaces (Autumn et al., 2006; Bullock and Federle, 2011; Dai et al., 2002; Gorb, 2011; Labonte and Federle, 2015; Wohlfart et al., 2014; Wolff and Gorb, 2013). On curved surfaces, opposing normal forces can be produced locally by contralateral limbs. Here, the magnitude of friction enhancement largely depends on surface curvature and leg morphology (Spinner et al., 2014; Voigt et al., 2017).

In the multi-articulated legs of arthropods, the lengths of tarsomeres, the number of joints and their range of movement determine how well the leg can follow the surface profile. This is crucial, as these animals are faced with extremely curved surfaces, such as thin plant stems or the edges of leaves (Gladun and Gorb, 2007; Voigt et al., 2017). Therefore, most terrestrial arthropods, such as insects, have evolved subdivided tarsi that can strongly bend ventrally to grip around rod-shaped structures (Frantsevich and Gorb, 2004; Gladun and Gorb, 2007; Walther, 1969).

Unparalleled tarsal flexion is accomplished by a group of arachnids: the long-legged harvestmen (Opiliones: Eupnoi). In these, tarsi can completely coil up and thus work as prehensile organs able to wrap around thin cylindrical objects like grass stems (Guffey et al., 2000; Kästner, 1931; Wolff and Gorb, 2016). This is achieved by extreme subdivision of tarsi: while insects have 3–7 tarsomeres, there can be more than 70 in phalangiid harvestmen (Wijnhoven, 2013). Tarsomeres are divided by adesmatic joints, i.e. secondary joints that are not controlled by muscles (Shultz, 1989; 2000). Flexion and extension of the tarsus is controlled by the pretarsus (claw) levator and depressor muscles, which are located in the patella and tibia and the basitarsus, respectively (Shultz, 1989, 2000). A system of pulleys guides the ventral tendon to keep proper motion control over the large number of adesmatic joints (Proud and Felgenhauer, 2013).

Unlike many insects and spiders, eupnoid harvestmen do not possess adhesive pads. Instead, the ventral sides of their prehensile tarsi are often densely covered with tapered hair-like protuberances (setae), which may generate friction by interlocking with minute asperities of natural surfaces (Wolff and Gorb, 2016). As the contact area of such structures with substrate surfaces is very limited, they presumably cannot generate sufficient adhesion to compensate for weight forces when walking on highly inclined smooth surfaces.

Here, we were interested in the performance of the prehensile system, to better understand the biomechanics of these specialised arthropod legs and their ecological implications. Furthermore, we identified this system as a potential model for the design of novel biomimetic grippers and robot legs, which further motivated this study. To study the effect of tarsal length on biomechanical performance, we chose three species of harvestmen (Arachnida: Opiliones: Eupnoi: Phalangioidea) that are frequently (but not exclusively) found on deciduous trees in Central Europe and differ in

[1]Functional Morphology and Biomechanics, University of Kiel, Am Botanischen Garten 1-9, 24098 Kiel, Germany. [2]Department of Biological Sciences, Macquarie University, Sydney, NSW 2109, Australia. [3]Department of Mechanical Engineering, Westphalian Institute for Biomimetics, University of Applied Sciences, Münsterstrasse 265, 46397 Bocholt, Germany. [4]Allgemeine und Spezielle Zoologie, Universität Rostock, Universitätsplatz 2, 18055 Rostock, Germany.

*Author for correspondence (jonas.wolff@mq.edu.au)

J.O.W., 0000-0003-2326-0326; A.K., 0000-0002-3338-0519

leg morphology and microhabitat use: (1) the short-legged *Paroligolophus agrestis* (Meade, 1855) (Phalangiidae), which is found on both branches and leaves; (2) the long-legged *Dicranopalpus ramosus* (Simon, 1909) (Phalangiidae), which prefers twigs and branches; and (3) the long-legged *Leiobunum blackwalli* (Meade, 1861) (Sclerosomatidae), which has a preference for leaves (J.O.W., personal observation) (Fig. 1C). Specifically, we addressed the following questions: (i) what is the morphological basis for extreme tarsal flexion?; (ii) how much can the tarsus be flexed and how well does it adapt to flat and cylindrical surfaces of different diameter?; (iii) can a harvestman scale smooth vertical surfaces without adhesive pads by traction enforcement?; (iv) how much does tarsal bending enhance traction?; and (v) is there an optimal substrate diameter at which traction forces are maximal?

We approached these questions by focusing on smooth glass surfaces, where claws cannot interlock and attachment is based on friction of setal soles of the tarsi.

MATERIALS AND METHODS
Animals
Adult harvestmen were collected from trees on and around the campus of the University of Kiel (Germany) and in Nijmegen (The Netherlands) using a beating tray. Collections were carried out in October, which is the peak season for the adult stage in the investigated species (adults can be found from August to February, depending on winter conditions). Animals were kept in plastic boxes (17×12×12 cm) lined on the base with moist paper tissue that was changed daily (conditions in boxes: 18–23°C, 60–80% relative humidity, natural light cycle from ambient light through windows). Harvestmen were fed twice per week with beetle jelly (Dragon Jelly Food, Dragon Terraristik, Duisburg, Germany) and pieces of dried mealworms.

All experiments with living animals complied with the German legislation for animal research. The species used are not legally protected under German law.

Tilting tests
To assess the attachment ability of harvestmen to smooth surfaces, tilting tests with 10 *P. agrestis* and 7 *D. ramosus* were performed. Animals were placed on horizontally aligned glass substrates fixed to a mechanical tilting platform. As substrates, conventional lab ware was used: a glass pane (200×200×4 mm; Erich Eydam KG, Kiel, Germany) and glass rods with diameters of 1.5 mm (tip of Pasteur pipette, length L=100 mm; Hirschmann Laborgeräte GmbH & Co. KG, Eberstadt, Germany), 4 mm (stirring rod, L=150 mm; Hedinger GmbH & Co. KG, Stuttgart, Germany) and 8 mm (stirring rod, L=250 mm; Carl Roth GmbH & Co. KG, Karlsruhe, Germany). Glass substrates were cleaned with absolute ethanol and acetone before use. The platform was inclined at approximately 1 deg s^{-1} from 0 deg (horizontal) to 180 deg (inverted). Movement was stopped if the animal began to slip off the surface, and the corresponding tilting angle measured as an indicator of attachment ability. Four runs were performed per individual and substrate, and their means calculated.

Traction force experiments
For traction force measurements, 4 female and 10 male *P. agrestis*, 4 female and 4 male *D. ramosus*, and 3 female and 5 male *L. blackwalli* were used. Prior to experiments, animals were weighed on an AG 204 Delta Range scale (Mettler Toledo GmbH, Greifensee, Switzerland). The experimental setup follows Wolff and Gorb (2012). Animals walked along horizontally positioned substrates (same substrate as in tilting tests plus a glass measuring cylinder with a diameter of 29.5 mm, L=256 mm; Duran
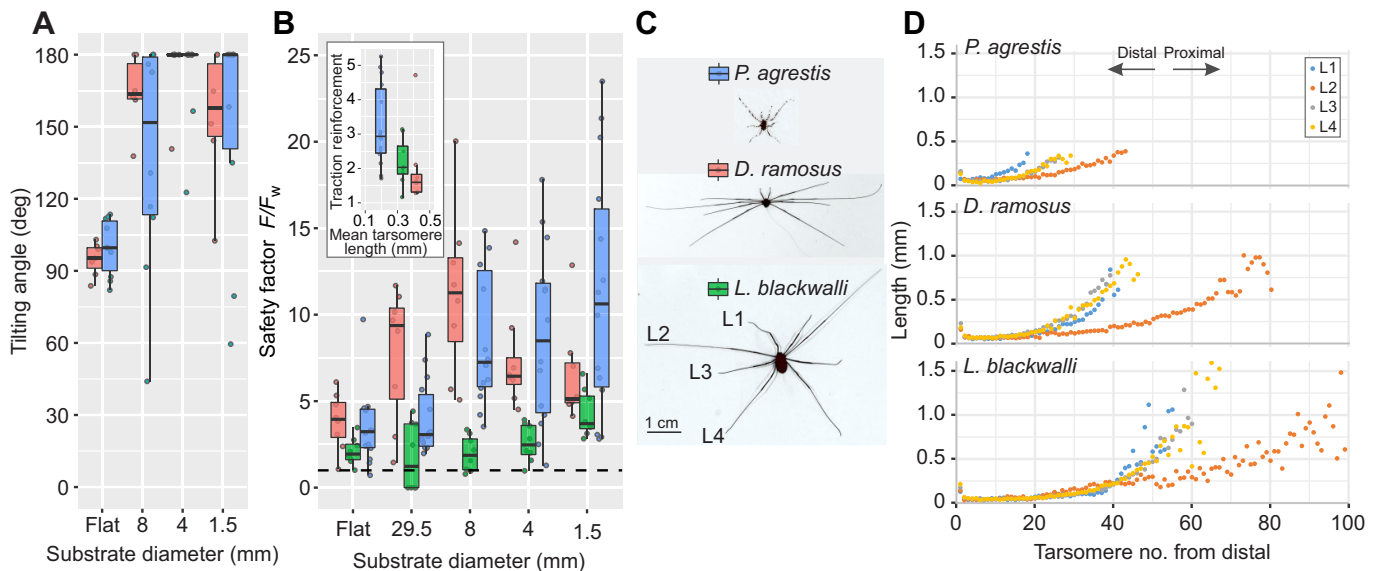
Fig. 1. Biomechanical performance and morphometrics of flexible tarsi in harvestmen. (A) Graphic representation of maximal tilting angles of *Paroligolophus agrestis* (blue; N=10 biological replicates) and *Dicranopalpus ramosus* (red; N=7) on flat and curved glass surfaces. Boxplots show the 25th and 75th percentiles of frictional adhesion angles; the thick line indicates the median; error bars define 1.5 times the inter-quartile range; remaining, out-of-range values are marked by circles. (B) Graphic representation of safety factors (traction force F divided by weight force F_w) from traction force measurements of *P. agrestis* (blue; N=14), *D. ramosus* (red; N=8) and *Leiobunum blackwalli* (green; N=8) on flat and curved glass surfaces. Boxplots display the safety factors [traction force (mN) divided by body weight (mN)], with the same conventions as in A. Inset shows the magnitude of traction forces (mN) on the 1.5 mm rod relative to traction forces (mN) on the flat substrate against mean tarsomere length. (C) Top view of exemplary individuals of the three species used, showing differences in size and relative leg length (L1–4). (D) Graphic representation of tarsomere length of left legs in an exemplary individual per species. Tarsomeres are numbered from distal to proximal (basitarsus omitted).

Group GmbH, Mainz, Germany; imprinted measurement scale was rotated downwards and could not be reached by the harvestmen). Substrates were presented in a randomised order.

Traction forces were transmitted to a FORT10-force transducer (World Precision Instruments, Inc., Sarasota, FL, USA) by means of a 10- to 15-cm-long human hair attached to the dorsal abdomen with a molten droplet of beeswax–colophonium compound. An escape response orthogonal to the load cell was triggered by lightly touching the animal's body with a brush. Maximal pulling forces were recorded using a Biopac MP-100 data acquisition system and AcqKnowledge 3.7.0 software (Biopac Systems Ltd, Goleta, CA, USA). Two runs per individual and substrate were performed and their mean used for statistical analysis to avoid pseudo-replication. The traction force normalised to body weight (safety factor) was compared between substrates and species using Kruskal–Wallis rank sum tests and all pairwise comparisons Wilcoxon tests in R 3.5.0 (http://www.R-project.org/). Safety factors were assessed in this analysis to reduce the effect of size differences of the species used.

Morphometrics

To quantify differences in leg articulation, the left walking legs of one exemplary female per species were detached at the trochanter and observed under an M205A stereo microscope (Leica Microsystems GmbH, Wetzlar, Germany). The length of each podomere and tarsomere was measured along the median line from micrographs using ImageJ 1.5 (Schneider et al., 2012).

These exemplary measurements did not take intraspecific and intersexual differences into account. This was previously investigated in detail for *D. ramosus* by Wijnhoven (2013), who found that mean leg length was about 25% higher in males than in females, with a standard deviation of about 5% within sexes (*N*=10 per sex), while tarsal length differed by 23% on average. This variation is below the interspecific difference in tarsal length reported here between both long-legged species and the short-legged *P. agrestis*.

Micro-computed tomography

For micro-computed tomography (μCT), walking legs of female *D. ramosus* and *L. blackwalli* were used. The specimens were fixed using Bouin's fixative and critical-point dried (Leica EM CPD00).

Specimens were mounted onto a specimen holder. X-ray imaging was performed using an XRadia Versa 410 X-ray microscope (Zeiss, Oberkochen, Germany) using the program Scout and Scan v.11 (40–60 kV, 150–200 μA, 2001–2701 projections, 5–20 s acquisition time).

Histology

Legs of female *D. ramosus* were fixed in Bouin's fixative. Dissected parts of the legs were dehydrated in ethanol or 2,2-dimethoxypropane and, after an intermediate step of epoxypropane, embedded in Araldite epoxy resin under vacuum. Semi-thin sections (1.0 μm) were made with a rotary microtome (Leica, RM 2165) using either glass or diamond knives and were stained for 40 s at 80°C in a mixture of 1% Azure II and 1% Methylene Blue in a 1% aqueous borax solution diluted 1:20 in Aqua Bidest. Serial semi-thin sections were digitalised using an Axio Imager.M1 (Zeiss) equipped with a Zeiss AxioCamICc 3 and AxioVs40 v.4.7.1.0 software, converted to 8-bit greyscale using IrfanView and aligned using Autoaligner x64 6.0 (Bitplane, Zurich, Switzerland).

Scanning electron microscopy

For the visualisation of tarsal surface structures, autotomised walking legs of a female *D. ramosus* were air dried and prepared for scanning electron microscopy (SEM). Dried samples were glued to stubs using carbon-rich sticky tape and sputter coated with 10 nm Au–Pd. Specimens were studied with a Hitachi S 4800 scanning electron microscope (Hitachi Ltd, Tokyo, Japan) at an acceleration voltage of 3.0 kV.

RESULTS
Functional morphology

In all three species, tarsal length was highest in the second pair of legs (L2), followed by L4, L3 and then L1. Tarsal length was comparable in *D. ramosus* (L1: 15.5 mm; L2: 32.4 mm; L3: 16.5 mm; L4: 23.5 mm) and *L. blackwalli* (L1: 16.7 mm; L2: 35.1 mm; L3: 17.9 mm; L4: 26.2 mm), but was only a quarter of these values in *P. agrestis* (L1: 2.7 mm; L2: 9.4 mm; L3: 5.0 mm; L4: 7.4 mm). Despite having a similar leg length, *L. blackwalli* exhibited a higher subdivision of the tarsus (L1: 56; L2: 100; L3: 61;
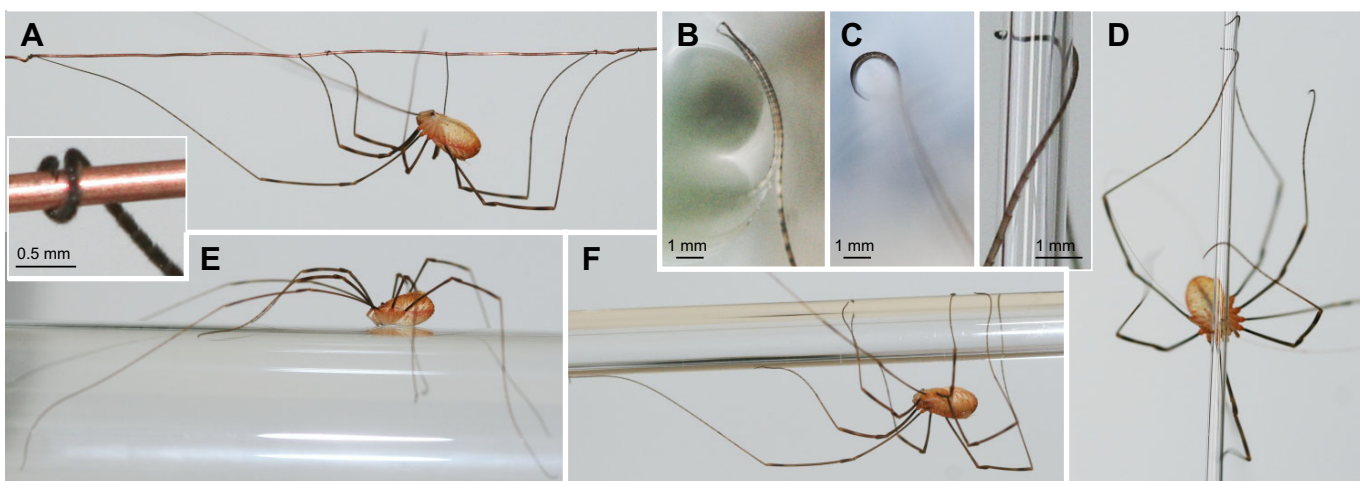
Fig. 2. Tarsus biomechanics on cylindrical objects. (A) *Leiobunum blackwalli* walking on 0.3 mm copper wire. Inset shows detail of left L1 exhibiting tarsal hyperflexion. (B) Detail of tarsus of *D. ramosus* on an 8 mm glass rod. (C) Detail of tarsus of *D. ramosus* on a 1.5 mm glass rod. (D) *Leiobunum blackwalli* climbing vertically on a 1.5 mm glass rod. Inset shows detail of left L4. (E) *Leiobunum blackwalli* walking on a glass cylinder of 29.5 mm diameter. (F) *Leiobunum blackwalli* walking on an 8 mm glass rod.

L4: 68 tarsomeres) than *D. ramosus* (L1: 43; L2: 81; L3: 40; L4: 47 tarsomeres). Tarsomere length exponentially increased from distal to proximal (Fig. 1E). Mean tarsomere length was shortest in *P. agrestis* (L1: 0.14 mm; L2: 0.21 mm; L3: 0.19 mm; L4: 0.25 mm), followed by *L. blackwalli* (L1: 0.30 mm; L2: 0.35 mm; L3: 0.29 mm; L4: 0.39 mm) and *D. ramosus* (length approximately doubled to L1: 0.36 mm; L2: 0.40 mm; L3: 0.41 mm; L4: 0.50 mm). The 10 most distal tarsomeres (excluding the distal-most tarsomere, which is always significantly longer and bears the pretarsus) were the shortest, with each having an average length of 65 µm in *P. agrestis* and *D. ramosus*, and 47 µm in *L. blackwalli*. This permits extremely narrow bending of the tarsal tip as observed in harvestmen walking on 0.3 mm copper wire (Fig. 2A).

µCT and histological results revealed the presence of a ventral and a dorsal tendon, with the former running through a system of sheaths (Fig. 3A–C). The adesmatic joints of the tarsal chain are dicondylous and articulate in the ventral direction. This is enabled by the trapeze-like shape of the tarsomeres, which are longer on the dorsal side than on the ventral side.

SEM of a leg of *D. ramosus* showed that the ventral side is densely covered in pointed setae (Fig. 3C,E), similar to what has been described in other eupnoid harvestman species (Wolff and Gorb, 2016).

Biomechanical performance

All three species of harvestmen showed significant differences in traction force on substrates with different curvature (*P. agrestis*: χ^2_4=21.153, *P*<0.001; *D. ramosus*: χ^2_4=16.284, *P*=0.003; *L. blackwalli*: χ^2_4=14.243, *P*=0.007) (Fig. 1B; Table S1). In the short-legged *P. agrestis*, traction was significantly enhanced on glass rods with a diameter of 8, 4 and 1.5 mm. In the long-legged *L. blackwalli*, the highest forces were obtained on the thinnest glass rod
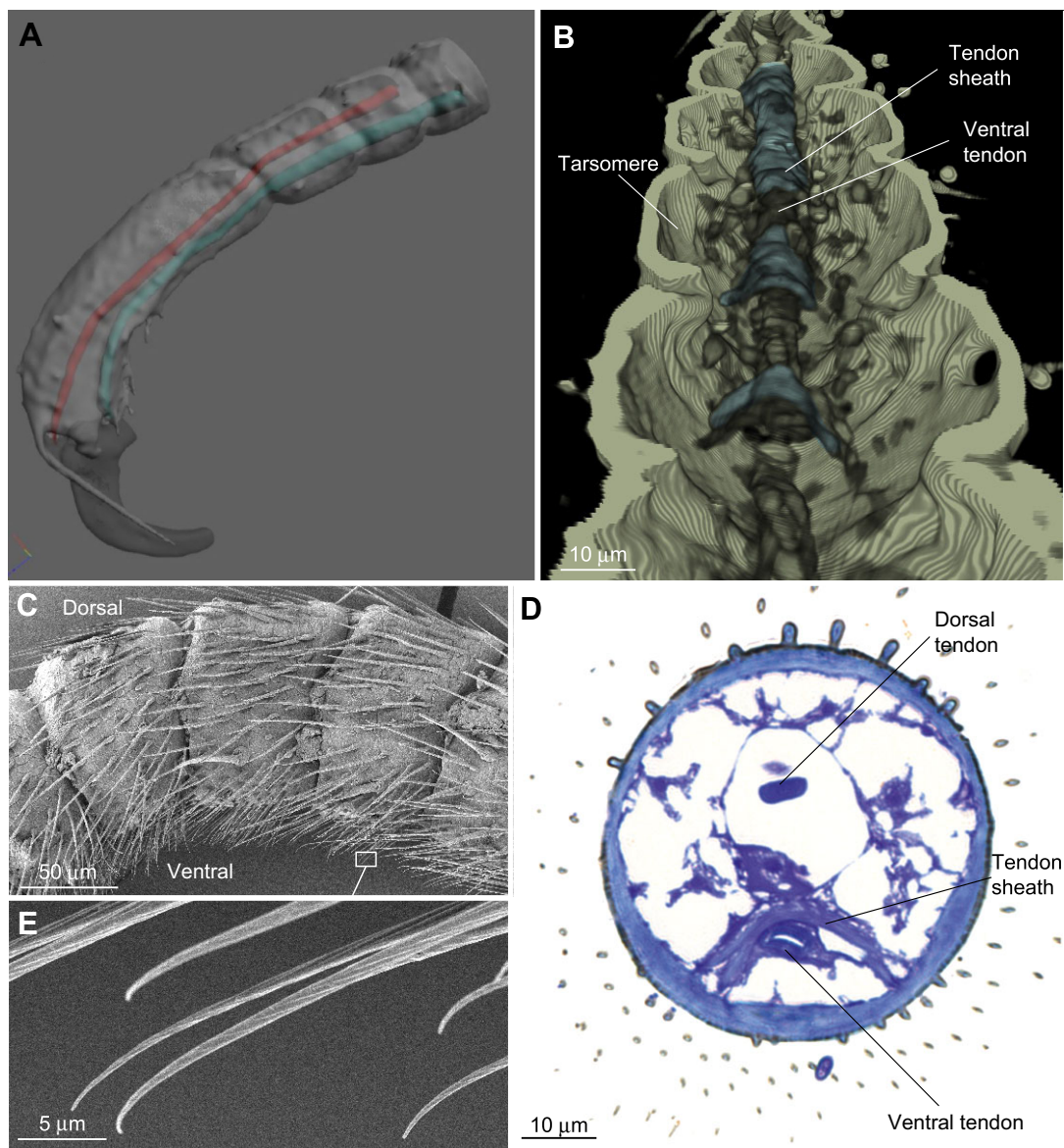
Fig. 3. Morphology of the opilionid tarsus. (A) 3D reconstruction of distal tarsus and pretarsus in *D. ramosus*. Pretarsal tendons are coloured. Download the pdf to activate interactive content. (B) Digital section of distal tarsus in *D. ramosus*, frontal plane, showing the pulley system of the ventral tendon. (C) Scanning electron micrograph of the distal tarsus of L4 of a female *D. ramosus*. (D) Histological cross-section of the distal tarsomere of L3 in a male *D. ramosus*. (E) Scanning electron micrograph of setal tips of the ventral tarsal sole of L4 of a female *D. ramosus*.

(diameter: 1.5 mm). In contrast, *D. ramosus* reached the highest forces on the 8 mm thick glass rod and traction was reduced on rods of smaller diameter. Traction reinforcement on the 1.5 mm thick rod (i.e. maximal traction force divided by maximal traction force on the rod on the flat glass surface) was increased in species with shorter mean tarsomere length (Fig. 1B, inset).

For all species, safety factor was above one on all substrates (except for three individuals of *L. blackwalli*, which could not establish a foothold on the 29.5 mm thick cylinder). While safety factor did not differ between species on the planar surface (χ^2_2=5.1553, P=0.076) and the thinnest glass rod (χ^2_2=6.2763, P=0.043; P>0.05 for all pairwise comparisons Wilcoxon tests), it did for all other curved surfaces. On the 29.5 mm glass cylinder, *D. ramosus* yielded the highest safety factors (χ^2_2=9.1438, P=0.010). On 4 mm (χ^2_2=12.737, P=0.002) and 8 mm (χ^2_2=17.461, P<0.001) thick glass rods, safety factors of *L. blackwalli* were significantly lower than those of the two other species.

Tilting experiments confirmed that *P. agrestis* and *D. ramosus* can hold their body weight on smooth vertical surfaces, with mean tilting angles of 100 deg on the flat substrate in both species. Tilting angles were higher on glass rods than on the flat glass surface (Fig. 1A). On the 8 mm thick rods, *D. ramosus* reached angles between 160 and 180 deg and *P. agrestis* reached angles between 45 and 180 deg. On the 4 mm rod, all but one *D. ramosus* and two *P. agrestis* stayed attached to full inversion (180 deg). On the 1.5 mm thick rod, in both species half of the harvestmen slipped off before the full inversion cycle was completed.

DISCUSSION

Our results confirm the hypothesis that eupnoid harvestmen can enhance traction on cylindrical objects by tarsal wrapping. Notably, this principle enables these animals to scale vertical smooth surfaces despite the lack of adhesive foot pads. Tarsal flexion enhances the contact area of setal soles and redirects normal forces by closely adapting to the surface curvature (Fig. 2). Normal forces can be controlled in each leg independently by the pretarsus muscles. A simple principle permits tarsal adaptability to an enormous range of surface curvature: tarsomere length decreases towards the tip, such that the foot exhibits a longitudinal flexibility gradient. This morphology also ensures that the foot does not deform in a chaotic manner when the pretarsal depressor contracts.

Our species comparison revealed that it is not the tarsal length but the degree of tarsus subdivision that plays the dominant role in surface adaptability and traction reinforcement. The observed differences can be explained by adaptations to the animal's microhabitat niche. *Dicranopalpus ramosus*, the species with the fewest articulations per length unit, is an ambush predator on twigs, where it rests in a characteristic posture with its legs laterally stretched along the branch. The curvature of these surfaces is comparably low when compared with, for example, leaf edges, ribs and petioles, which both of the other species frequently walk on (J.O.W., personal observation).

Foot adaptability to curved surfaces may have far-reaching ecological consequences. For birds (e.g. reed warblers), primates and chameleons, it has been shown that foot morphology and gripping strength correlate with perch diameter (Leisler et al., 1989; Lemelin, 1999; Silva et al., 2014), indicating selective pressures on foot mechanics. However, evolutionary constraints due to genealogical history (phylogenetic burden), like the fixed number of joints in vertebrate toes, severely restrict the eco-morphological space. This may constrain niche occupation. For instance, in contrast to arachnids, insects only possess a single pretarsal tendon. This means that tarsal extension can only be performed by passive mechanisms, like the release of stored elastic energy, which may become increasingly difficult the more tarsal joints are introduced. This may constrain the evolution of tarsal length and tarsus subdivision. As a consequence, insects cannot hyperflex their tarsi to form a full loop, limiting surface adaptability, contact area and normal force enhancement (Gladun and Gorb, 2007). Accordingly, rod-shaped structures like plant stems are challenging substrates for many insects (Gladun and Gorb, 2007). Some invertebrates exploit this limitation and place exposed eggs on thin secreted stalks to exclude insect predators (Růžička, 1997). Similarly, insect herbivory could be an evolutionary driver for plant stem and petiole thinness, a largely overlooked aspect in the evolutionary ecology of insect–plant interactions. Harvestmen have overcome some of these limitations, enabling them to manoeuvre through complex terrain even without the use of tarsal adhesive pads or secretions.

The prehensile feet of harvestmen are unique among animals. In contrast to the prehensile systems of vertebrates (e.g. prehensile tails or elephant trunks), molluscs (octopus arms) and worms, harvestman feet can undergo a multitude of deformations with only two 1D actuators. This renders them a very attractive model for biomimetic engineering of underactuated robotic devices, such as surgical probes, grippers and transportation systems. To date, harvestman locomotion has drawn the interest of robotic engineers because of their outstanding manoeuvrability in complex terrain (Hodoshima et al., 2016, 2013). However, so far these studies have focused on body to leg length ratios and have omitted the most interesting aspects of harvestman locomotion based on tarsus flexibility. Our work may thus trigger new innovations.

Author contributions
Conceptualization: J.O.W.; Methodology: J.O.W., C.S.W.; Validation: J.O.W.; Formal analysis: J.O.W., C.W., C.S.W.; Investigation: C.W., C.S.W., A.K.; Resources: C.S.W., S.N.G.; Data curation: C.W., C.S.W., S.N.G.; Writing - original draft: J.O.W., C.W.; Writing - review & editing: C.S.W., S.N.G.; Visualization: J.O.W., C.S.W.; Supervision: J.O.W., S.N.G.; Project administration: J.O.W.; Funding acquisition: J.O.W.

References
Autumn, K., Dittmore, A., Santos, D., Spenko, M. and Cutkosky, M. (2006). Frictional adhesion: a new angle on gecko attachment. *J. Exp. Biol.* **209**, 3569-3579.

Bußhardt, P., Kunze, D. and Gorb, S. N. (2014). Interlocking-based attachment during locomotion in the beetle Pachnoda marginata (Coleoptera, Scarabaeidae). *Sci. Rep.* **4**, 1-8.

Bullock, J. M. R. and Federle, W. (2011). The effect of surface roughness on claw and adhesive hair performance in the dock beetle Gastrophysa viridula. *Insect Sci.* **18**, 298-304.

Dai, Z., Gorb, S. N. and Schwarz, U. (2002). Roughness-dependent friction force of the tarsal claw system in the beetle Pachnoda marginata (Coleoptera, Scarabaeidae). *J. Exp. Biol.* **205**, 2479-2488.

Endlein, T., Ji, A., Yuan, S., Hill, I., Wang, H., Barnes, W. J. P., Dai, Z. and Sitti, M. (2017). The use of clamping grips and friction pads by tree frogs for climbing curved surfaces. *Proc. R. Soc. B* **284**, 20162867.

Frantsevich, L. and Gorb, S. (2004). Structure and mechanics of the tarsal chain in the hornet, Vespa crabro (Hymenoptera: Vespidae): implications on the attachment mechanism. *Arthropod. Struct. Dev.* **33**, 77-89.

Gladun, D. and Gorb, S. N. (2007). Insect walking techniques on thin stems. *Arthropod Plant Interact.* **1**, 77-91.

Gorb, S. N. (2011). Biological fibrillar adhesives: functional principles and biomimetic applications. In *Handbook of Adhesion Technology* (ed. L. F. M. da Silva, A. A. Öchsner and R. D. Adams), pp. 1409-1436. Berlin: Springer.

Guffey, C., Townsend V. R., , Jr and Felgenhauer, B. E. (2000). External morphology and ultrastructure of the prehensile region of the legs of Leiobunum nigripes (Arachnida, Opiliones). *J. Arachnol.* **28**, 231-236.

Hodoshima, R., Watanabe, S., Nishiyama, Y., Sakaki, A., Ohura, Y. and Kotosaka, S. (2013). Development of ASURA I: harvestman-like hexapod walking robot—approach for Long-legged robot and leg mechanism design. In Intelligent Robots and Systems (IROS), 2013 IEEE/RSJ International Conference on, pp. 4669-4674: IEEE.

Hodoshima, R., Ohura, Y., Nishiyama, Y., Sakaki, A., Watanabe, S. and Kotosaka, S. (2016). The ASURA I harvestman-like hexapod walking robot: compact body and long leg design. *Adv. Robot.* **30**, 1467-1483.

Kästner, A. (1931). Biologische Beobachtungen an Phalangiiden. *Zool. Anz.* **95**, 293-302.

Labonte, D. and Federle, W. (2015). Scaling and biomechanics of surface attachment in climbing animals. *Phil. Trans. R. Soc. B* **370**, 20140027.

Leisler, B., Ley, H.-W. and Winkler, H. (1989). Habitat, behaviour and morphology of Acrocephalus warblers: an integrated analysis. *Ornis Scand.* 181-186.

Lemelin, P. (1999). Morphological correlates of substrate use in didelphid marsupials: implications for primate origins. *J. Zool.* **247**, 165-175.

Meade, R. H. (1855). Monograph on the British Species of Phalangiidae or Harvestmen. *Ann. Mag. Nat. Hist.* **15**, 393-416.

Meade, R. H. (1861). Supplement to a monograph on the British species of Phalangiidae, or harvest-man. *Ann. Mag. Nat. Hist.* **7**, 353-354.

Proud, D. N. and Felgenhauer, B. E. (2013). The harvestman tarsus and tarsal flexor system with notes on appendicular sensory structures in Laniatores. *J. Morphol.* **274**, 1216-1229.

Ružička, Z. (1997). Protective role of the egg stalk in Chrysopidae (Neuroptera). *Eur. J. Entomol.* **93**, 161-166.

Schneider, C. A., Rasband, W. S. and Eliceiri, K. W. (2012). NIH Image to ImageJ: 25 years of image analysis. *Nat. Methods* **9**, 671-675.

Shultz, J. W. (1989). Morphology of locomotor appendages in Arachnida: evolutionary trends and phylogenetic implications. *Zool. J. Linn. Soc.* **97**, 1-55.

Shultz, J. W. (2000). Skeletomuscular anatomy of the harvestman Leiobunum aldrichi (Weed, 1893) (Arachnida: Opiliones: Palpatores) and its evolutionary significance. *Zool. J. Linn. Soc.* **128**, 401-438.

Silva, J. M., Herrel, A., Measey, G. J., Vanhooydonck, B. and Tolley, K. A. (2014). Linking microhabitat structure, morphology and locomotor performance traits in a recent radiation of dwarf chameleons. *Funct. Ecol.* **28**, 702-713.

Simon, E. (1909). Étude sur les Arachnides recueillis au Maroc par M. Martínez de la Escalera en 1907. *Memorias de la Real Sociedad Española de Historia Natural* **6**, 5-43.

Spinner, M., Westhoff, G. and Gorb, S. N. (2014). Subdigital setae of chameleon feet: friction-enhancing microstructures for a wide range of substrate roughness. *Sci. Rep.* **4**, 5481.

Voigt, D., Takanashi, T., Tsuchihara, K., Yazaki, K., Kuroda, K., Tsubaki, R. and Hosoda, N. (2017). Strongest grip on the rod: tarsal morphology and attachment of Japanese pine sawyer beetles. *Zoological Lett.* **3**, 16.

Walther, C. (1969). Zum Verhalten des Krallenbeugersystems bei der Stabheuschrecke Carausius morosus Br. *Zeitschrift Fur Vergleichende Physiologie* **62**, 421-460.

Wijnhoven, H. (2013). Sensory structures and sexual dimorphism in the harvestman Dicranopalpus ramosus (Arachnida: Opiliones). *Arachnol. Mitt.* **46**, 27-46.

Wohlfart, E., Wolff, J. O., Arzt, E. and Gorb, S. N. (2014). The whole is more than the sum of all its parts: collective effect of spider attachment organs. *J. Exp. Biol.* **217**, 222-224.

Wolff, J. O. and Gorb, S. N. (2012). The influence of humidity on the attachment ability of the spider Philodromus dispar (Araneae, Philodromidae). *Proc. R. Soc. B Biol. Sci.* **279**, 139-143.

Wolff, J. O. and Gorb, S. N. (2013). Radial arrangement of Janus-like setae permits friction control in spiders. *Sci. Rep.* **3**, 1101.

Wolff, J. O. and Gorb, S. N. (2016). *Attachment Structures and Adhesive Secretions in Arachnids*. Cham, Switzerland: Springer International Publishing.

Table S1. Raw data of traction force measurements.

Click here to Download Table S1